Available online at www.sciencedirect.com
ScienceDirect
Computer Physics Communications 177 (2007) 72–75
Computer Physics Communications
www.elsevier.com/locate/cpc

Low-pressure plasma generation inside slender tubes

F. Iza, J.K. Lee *

Department of Electronics and Electrical Engineering, Pohang University of Science and Technology, Pohang 790-784, Republic of Korea

Available online 28 February 2007

Abstract

Low pressure (<50 mTorr) argon discharges inside tubes of a few millimeters in diameter have been studied by means of one- and two-dimensional particle-in-cell Monte Carlo collision simulations. Magnetically confined DC and microwave discharges have been sustained in a coaxial configuration. For DC discharges, the magnetic field needs to be strong enough to confine secondary electrons emitted from the cathode, i.e. the amplitude of the cycloidal motion described by secondary electrons has to be smaller than the discharge gap. For microwave excited discharges, the power absorption profile depends on the magnitude of the magnetic field. Power absorption beyond the sheath boundary in the plasma bulk and better confinement for magnetic fields below the ECR condition lead to maximum densities at $\omega_c/\omega_{rf} \sim 0.5$.

Keywords: ECR plasma; Coaxial magnetron; Magnetized discharge; Inner wall; Slender tube

1. Introduction

Being able to plasma-treat the inner wall of slender tubes is desirable to improve the performance of tubes and other instruments in biomedical and industrial applications [1,2]. For example, treatment and coating of catheters can improve their biocompatibility and fouling properties. Similarly, a coating can improve the lifetime of pipes that will carry corrosive materials.

Various techniques/configurations have been used in the past to treat the inner wall of tubes. Electro-explosion [3], ion beams and movable targets [4], external discharges [5], plasma immersion ion implantation [6], and magnetized discharges [7] provide means of treating the inner wall of slender tubes with different performance in terms of repeatability, uniformity and throughput.

This paper studies low-pressure (<50 mTorr) argon discharges inside tubes of inner radii on the order of millimeters. The discharges are sustained between the tubes and auxiliary wires introduced inside the tubes, i.e. coaxial configuration. A detailed description of experimental set-ups can be found in [8,9]. One- and two-dimensional particle-in-cell Monte Carlo (PIC-MCC) collision simulations have been performed to study the plasma characteristics under various magnetic field intensities and driving schemes. PIC-MCC simulations capture particle kinetics without the assumptions required in fluid models and have been successfully used in studies of fundamental and applied plasma physics [11]. The simulation results provide a new insight into the underlying physics and are in good agreement with experimental data.

2. Simulation model and device description

The discharges are sustained in a coaxial configuration. The tube being treated acts as the outer electrode and a thin wire introduced inside the tube as the inner electrode. For a sputter-coating application, the thin wire is made of the coating material and it is negatively biased so that the ion bombardment sputters it. DC, pulsed-DC and microwave discharges can be used to coat metallic and dielectric tubes [8,9]. In order to effectively accelerate ions against the inner electrode (target) operation at low pressure is required. Typically, this pressure is below 50 mTorr and therefore magnetic confinement is needed to limit the particle loss to the tube walls.

Simulations results are obtained using XPDC1 [12], an open-source one-dimensional (1d3v) PIC-MCC code, and a two-dimensional (2d3v) axisymmetric PIC-MCC plasma simulator (APPS) developed by the authors. APPS assumes azimuthal symmetry and solves for the radial and axial profiles. A multigrid solver is used to determine the electrostatic

* Corresponding author.
E-mail address: jkl@postech.ac.kr (J.K. Lee).

0010-4655/$ – see front matter
doi:10.1016/j.cpc.2007.02.069

field and a leap-frog scheme to integrate the particles equations of motion. The code incorporates an external circuit and Poisson's equation is solved on a uniform grid using superposition of surface and volume charge densities. A few million particles and a radially weighted filter are used to minimize numerical noise. Elastic, excitation and ionization electron-neutral collisions, and elastic and charge exchange ion-neutral collisions are considered in the models (see [11,13] and references within). Coulomb collisions are not included in the model and therefore the effective electron temperature may be underestimated. Heating of low energy electrons intrinsic to PIC-MCC simulations, however, may partially compensate for physical coulomb interactions [14].

For discharges run in DC mode, the secondary electron emission coefficient for Ar^+ ions impinging on the electrodes is set to 0.2 whereas no secondary electrons are considered in the microwave case. Finally, the magnetic field is assumed to be uniform across the discharge.

3. Simulation results

3.1. DC excitation

When the discharge is sustained in DC mode, the tube and the inner electrode constitute a coaxial magnetron. In the absence of a magnetic field, most secondary electrons emitted from the inner electrode transit the discharge gap without colliding with the background gas and therefore it is not possible to sustain a discharge inside the tube. If a sufficiently strong axial magnetic field is applied, however, electrons are turned around by the Lorentz force before reaching the tube. Confined secondary electrons describe circular cycloids spending longer time inside the tube and increasing the chances of undergoing collisions. The amplitude of the cycloids increases as the inner electrode diameter decreases [13] and therefore, there exists an optimum inner electrode diameter that minimizes the required magnetic field to sustain the discharge inside a given tube.

The electron energy probability function measured in the bulk plasma shows two distinct electron populations: high energy electrons that have been accelerated across the cathode fall, and low energy electrons that have been born in the bulk plasma. The high energy electrons are secondary electrons emitted from the inner electrode. These electrons ionize the background gas generating low energy electrons. These low-energy electrons diffuse very slowly in the radial direction and as a result, a high-density low-temperature plasma is obtained [13].

Most ions bombarding the inner electrode transit the sheath without colliding with the background gas, and therefore the ion energy distribution function presents a single energy peak. This energy corresponds to the sheath voltage (∼950 V when the applied voltage is 1 kV). Since the sheath is collisionless, ions strike the inner electrode almost perpendicularly. Some secondary electrons are also recaptured by the inner electrode. See Fig. 1.

Electrons arrive to the tube with a broad angular distribution and relatively large energy (∼25 V). A small number of

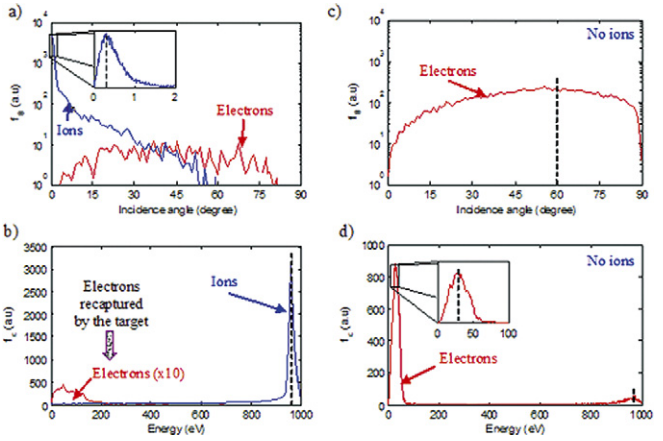

Fig. 1. (a) Angle and (b) energy distribution functions of electrons and ions impinging on the inner electrode. (c) Angle and (d) energy distribution functions of electrons and ions impinging on the tube.

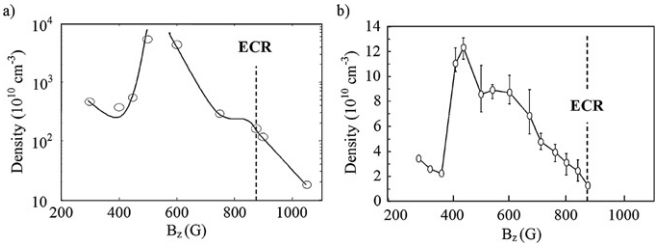

Fig. 2. Plasma density at the center of the discharge. (a) Simulation results: Applied voltage 30 V–2.45 GHz. (b) Experimental data [10]: $P = 30W - 2.45$ GHz.

electrons arrive to the tube with energies close to the applied voltage. These electrons are secondary electrons that have undergone a collision and have been deflected from their cycloidal orbits.

Since the axial diffusion of particles is not affected by the magnetic field, particle losses across the open-ends of the tube can be even larger than radial losses. Two-dimensional simulations modeling different configurations at the open end show that despite the slender geometry of the tube the discharge cannot be sustained without some axial confinement. Axial confinement, either electrostatic or magnetic, not only enables the discharge and higher plasma densities, but it also improves the uniformity of the plasma treatment [13].

3.2. Microwave excitation

In this section we present simulation results obtained when a 2.45 GHz voltage source is used to power up the inner electrode. Fig. 2 shows the plasma density at the center of the discharge as a function of the magnetic field for an argon discharge in a tube of radius 4 mm and an inner electrode of radius 500 μm. Despite the resonant heating occurring at the electron cyclotron resonance (ECR) condition ($B \sim 875$ Gauss), higher plasma densities are obtained when weaker magnetic fields are used.

Under ECR conditions, electrons are resonantly accelerated and may spiral out of the gap without undergoing collisions.

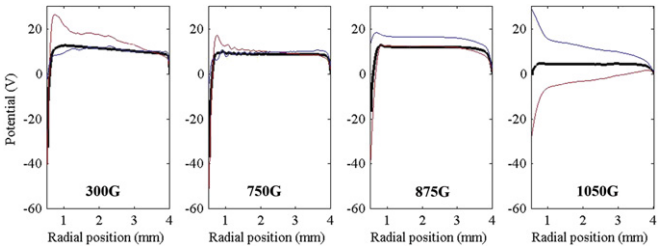

Fig. 3. Potential profiles: Time averaged (thick black line) and instantaneous profiles (thin colored lines) when the potential of the inner electrode is at its maximum and minimum value. (For interpretation of the references to color in this figure legend, the reader is referred to the web version of this article.)

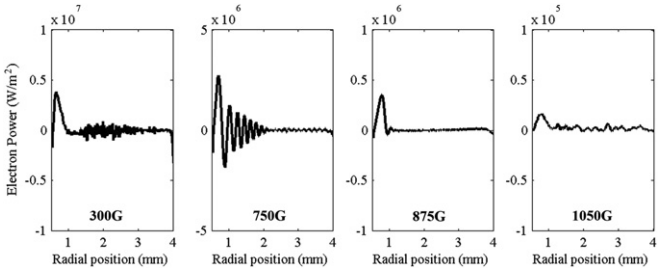

Fig. 4. Time averaged electron power ($2\pi r J_e(r,t) \cdot E(r,t)$) deposition profiles.

A confinement argument, however, cannot explain the rapid increase of plasma density as the magnetic field approaches $\omega_c/\omega_{rf} \sim 0.5$ nor the density decrease when the magnetic field is increased above the ECR condition. Here ω_c is the electron cyclotron frequency and ω_{rf} the excitation frequency (2.45 GHz).

Fig. 3 shows the radial potential profile for various magnetic field intensities. Similarities can be found with the more studied case of magnetically enhanced reactive ion etchers (RIE) [15]. As the magnetic field increases, the cross-field electron mobility decreases and the plasma becomes more resistive. The reduction of electron mobility results in a reduction (in absolute value) of the bias voltage. With high magnetic fields (see the 1050G case in Fig. 3), the inner electrode can reach instantaneously voltages above the plasma potential and large voltage drops are sustained across the bulk plasma. Nonetheless, an important difference with respect to magnetically enhanced RIEs should be noted. Besides the geometrical configuration, magnetically enhanced RIEs operate typically with magnetic fields well above the ECR condition. In this paper, however, the magnetic field intensity is such that the electron cyclotron frequency is also smaller than the excitation frequency.

Fig. 4 shows the time averaged electron power absorption profile as a function of the radial position. The electron power is defined as $J_e \cdot E$, where J_e is the electron current density and E the electric field. Significant changes can be observed in the power absorption profiles.

For high magnetic fields (1050G, above the ECR condition), the electron heating takes place at the sheath–plasma boundary near the inner electrode (Fig. 4). The time resolved data (not shown) indicates that the electron current is almost 90 degrees out of phase with respect to the electric field and that the current leads the electric field, i.e. the bulk plasma behaves capacitively. Although unmagnetized low pressure plasmas behave inductively due to the electron inertia, in a magnetized discharge above the ECR condition ($\omega_c > \omega_{rf}$) the Lorentz force makes particles turn before the electric field reverses. This leads to the capacitive behavior. Since electrons cross-field mobility is limited, stochastic heating at the sheaths is negligible and the net power absorption observed in Fig. 4 is due to collisional heating (no power is absorbed if collisions are artificially removed in the simulation). Although the average power deposition profile is similar for the ECR condition ($B = 875$G), the time evolution is quite different. Furthermore, at ECR the power is absorbed collisionlessly (power is absorbed even if the collisions are artificially removed in the simulation). For magnetic fields such that $\omega_c/\omega_{rf} \approx 0.5$–1, the power deposition profile presents a radial standing wave pattern with alternating layers of positive and negative power absorption. As a result, power is absorbed beyond the sheath–bulk interface. It is believed that the power absorption inside the bulk plasma is responsible for the enhanced plasma density observed in the simulation and experimental data (Fig. 2). As the magnetic field is reduced to 300G, electrons gain mobility and the discharge recovers the typical characteristics of an unmagnetized capacitive discharge.

4. Conclusions

Low pressure (<50 mTorr) plasma generation inside tubes of a few millimeters in diameter has been studied by means of one- and two-dimension particle-in-cell Monte Carlo collision simulations. The large particle loss to the tube wall at low pressure requires the use of magnetic confinement. DC and microwave argon discharges operated in a coaxial configuration have been analyzed and good agreement is found with existing experimental data. Despite the resonant heating occurring at the electron cyclotron resonance (ECR) condition, this is not the best operation point for discharges inside slender tubes. Poor particle confinement under the ECR condition and enhanced power absorption in the bulk plasma at lower magnetic fields result in higher plasma densities at $\omega_c/\omega_{rf} \sim 0.5$. For magnetic fields such that $\omega_c/\omega_{rf} = 0.5$–1 a radial standing wave pattern in the power absorption profile has been shown. Although not all the elements of this profile are yet understood, this power absorption profile indicates that power is delivered beyond the sheath–plasma interface into the bulk plasma.

Acknowledgements

This work was supported by the Korean Ministry of Education through its Brain Korea 21 program and the Korean Science and Engineering Foundation under Grant No. R11-2000-086-0000-0.

References

[1] M.A. Lieberman, A.J. Lichtenberg, Principles of Plasma Discharges and Materials Processing, second ed., John Wiley & Sons Inc., New York, 2005.

[2] C.M. Chan, T.M. Ko, H. Hiraoka, Surface Science Reports 24 (1999) 1.
[3] M. Batalov, P.S. Mohanty, ASM Materials solutions conference and show, Columbus OH, 2004.
[4] W. Ensinger, et al., Surface Coatings Technol. 150 (2002) 227.
[5] J.L. Lauer, J.L. Shohet, R.M. Albrecht, S. Esnault, J.S. Malter, U.H. von Andrian, S.B. Shohet, IEEE Trans. Plasma Sci. 33 (2005) 791.
[6] Liu, et al., J. Vacuum Sci. Technol. A 19 (2001) 2958.
[7] R. Hytry, W. Muller, R. Wilhelm, Surface Coatings Technol. 74–75 (1995) 43.
[8] H. Fujiyama, Surface Coatings Technol. 131 (2000) 278.
[9] T. Nagano, H. Fujiyama, Jpn. J. Appl. Phys. 38 (1999) 4338.
[10] H. Inoue, Y. Furue, H. Fujiyama, in: 7th Asian Pacific Conference on Plasma Science and Technology (Fukuoka, Japan, 2004).
[11] H.C. Kim, F. Iza, S.S. Yang, M. Radmilovic-Radjenovic, J.K. Lee, J. Phys. D: Appl. Phys. 38 (2005) R283.
[12] J.P. Verboncoeur, M.V. Alves, V. Vahedi, C.K. Birdsall, J. Comp. Phys. 104 (1993) 321.
[13] F. Iza, S.H. Lee, J.K. Lee, in: J. de Amorim Filho (Ed.), Computer Modeling of Low-Temperature Plasmas in Gas discharges (Research Signpost), submitted for publication.
[14] M. Turner, Physics of Plasmas 13 (2006) 033506.
[15] M. Kushner, J. Appl. Phys. 94 (2003) 1436.